

Out-of-plane Enhanced Magnetic Anisotropy Energy in Ni_3Bz_3 molecule

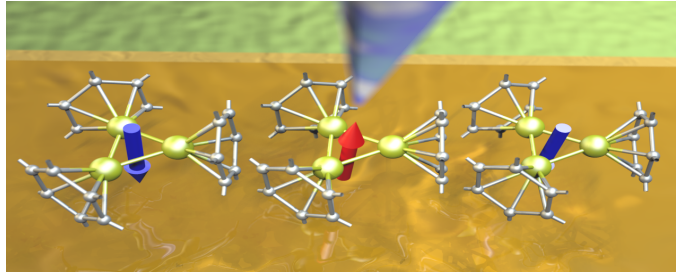
T. Alonso-Lanza^{1,*}, J. W. González^{1,†}, F. Aguilera-Granja^{1,2}, A. Ayuela¹

⁽¹⁾ *Centro de Física de Materiales (CSIC-UPV/EHU)-Material Physics Center (MPC), Donostia International Physics Center (DIPC), Departamento de Física de Materiales, Fac. Químicas UPV/EHU. Paseo Manuel de Lardizabal 5, 20018, San Sebastián-Spain.*

⁽²⁾ *Instituto de Física, Universidad Autónoma de San Luis Potosí, 78000 San Luis Potosí, México.*

(Dated: June 30, 2021)

Organometallic complexes formed by transition metals clusters and benzene molecules have already been synthesized, and in selected cases display magnetic properties controlled by external magnetic fields. We have studied Ni_nBz_n complexes made of nickel atoms surrounded by benzene molecules and here we focus specifically on the magnetic molecule Ni_3Bz_3 . By means of calculations including relativistic spin-orbit terms, we show that this molecule reveals a large magnetic anisotropy energy of approximately 8 meV, found with the easy axis perpendicular to the metal atoms plane. Note that the matching bare Ni_3 cluster have similar magnetic anisotropy, however the easy axis is in-plane. Covering with benzene molecules is thus switching the easy axis from in-plane for Ni_3 to out-of-plane for Ni_3Bz_3 . The large out-of-plane magnetic anisotropy of Ni_3Bz_3 suggests that this molecule could indeed be used as part in the design of molecular magnetic memories.



I. INTRODUCTION

The interaction of transition metal atoms with organics molecules have attracted much interest in theoretical and experimental studies since the synthesis of ferrocene¹. Related complexes known as metallocenes are formed by replacing iron with other transition metals^{2–4}, and have widespread importance in a wide range of applications, such as spintronics^{5–7}, biomedical products^{8,9}, and solar cells efficiency^{10–12}. Complexes formed by benzenes (Bz) and first-row transition metal atoms are currently being considered^{13–18}. Among those, experiments are discovering and synthesizing a large number of nickel-benzene complexes, which are later characterized by photoelectron spectroscopy^{19,20}. The simplest unit in these compounds, NiBz , places the nickel atom over a benzene hollow site^{21,22}. The ground state structure for metallocene NiBz_2 shows the Ni atom attached in a bridge site between carbon-carbon bonds in Bz molecules, that are then being shifted^{22–25}. However, experiments indicate that large Ni-Bz compounds adopt the so-called riceball structure, in which Ni atoms are wrapped by Bz molecules²⁰.

Magnetic effects in benzene transition metal complexes

are remarkable and of particular interest for applications. For instance, non-collinear magnetic orders for Co_3Bz_3 have been found²⁶, magnetism depletion is observed in manganese-benzene compounds²⁷, and it has been proposed that cobalt dimers on benzene may be magnetic storage bits²⁸. Early transition atoms such as Sc, V and Ti when they are placed over benzene molecule enhance magnetic moments, others such as Mn, Fe and Co atoms decrease magnetic moments, and Ni atom magnetic moment is totally quenched¹⁵. Previous works on Ni-Bz complexes²⁹ showed that caging small nickel clusters with benzene molecules fully deplete the magnetism in most of the cases, such as NiBz , NiBz_2 , Ni_2Bz_2 and Ni_3Bz_2 . The magnetism of bare nickel clusters was partially kept for cases, such as for Ni_2Bz and Ni_3Bz , when nickel-benzene rate is largely above one. As the size of the encapsulated nickel cluster increases the magnetic moment is more easily retained; Ni_3Bz_3 molecule preserves the magnetic moment of the bare nickel cluster. Here we focus on Ni_3Bz_3 because it is the smallest Ni-Bz complex retaining magnetism.

In this paper we investigate the structural and magnetic properties focusing on Ni_3Bz_3 complex by means of density functional calculations including spin-orbit interaction. The complex shows magnetism, keeping the same spin magnetic moment as for Ni_3 cluster. First we find the ground state of Ni_3Bz_3 molecule among different magnetic arrangements. Benzene molecules strongly affect the magnetic properties of the bare Ni_3 counter-

*Corresponding author: tomas.alonso001@ehu.eus

†Corresponding author: sgkgosaj@ehu.eus

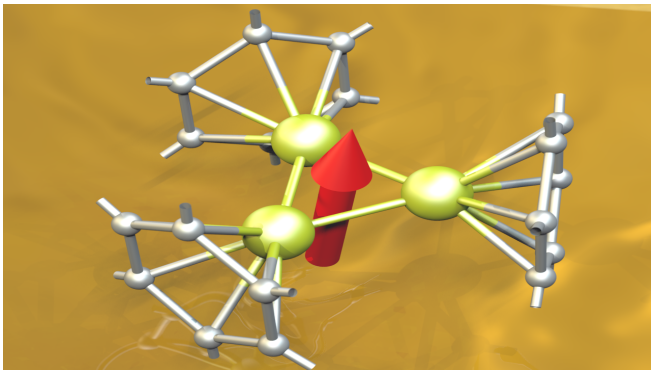


FIG. 1: Sketch of the ground state geometry of Ni_3Bz_3 molecule. The red arrow represents the easy axis of magnetization. The large out-of-plane anisotropy observed in these molecules enables a possible application as molecular magnetic storage units.

part, specifically the magnetic anisotropy. The two systems show a large magnetic anisotropy energy of approximately 8 meV, much larger than bulk Ni value in the order of few μeV per atom. However, the easy axis of magnetization switches from in-plane for Ni_3 to out-of-plane for Ni_3Bz_3 induced by benzene molecules. The large out-of-plane anisotropy in the Ni_3Bz_3 complexes may enable a possible application as molecular magnetic storage units, as sketched in Fig. 1.

II. METHODS

We perform density functional theory calculations using different methods. Spin polarized calculations of Ni-Bz complexes are performed using Vienna ab-initio simulation package (VASP), based on the projected augmented wave method^{30,31}. For the exchange and correlation potentials we used the Perdew-Burke-Ernzenhof form of the generalized gradient approximation³². We relax the structures of Ni_3Bz_3 and the Ni_3 molecules. A cut-off energy of 400 eV for plane wave basis set is used. We choose a cubic unit cell with sides 30 Å because such a cell is large to avoid interactions between images. For the calculations we use a Γ -point sampling. The molecule coordinates are relaxed until the atomic forces are less than 0.006 eV/Å. The results were also reproduced using the SIESTA method³³. The atomic cores were described by nonlocal norm-conserving relativistic Troullier-Martins pseudopotentials³⁴ with non-linear core corrections factorized in the Kleyman-Bylander form^{35,36}. We use an electronic temperature of 25 meV and a mesh-cutoff of 250 Ry.

For the geometry obtained with VASP, we study the effect of the spin-orbit interaction on the different magnetic configurations using the all-electron accurate full-potential linearized augmented plane-wave (FP-LAPW) method as implemented in ELK software³⁷⁻³⁹. To include the non-collinearity the electronic exchange-

correlation potential is treated within local spin density approximation⁴⁰. Wavefunctions, density, and potential in FP-LAPW calculations are expanded in spherical harmonics within spheres and in plane waves in the interstitial region. We use a plane-wave cut-off of $K_{\text{max}}R_{\text{Ni}} = 15$, where $R_{\text{Ni}} \approx 1.1$ Å is the nickel muffin-tin radius. The local magnetic moments are set in particular directions by applying small initial magnetic fields that decrease in each self-consistent loop as to be negligible³⁸. Calculations use now 15 Å of empty space to avoid interactions between nearest-neighbor cells.

We are performing state-of-the-art all electron relativistic calculations including non-collinearity, with spin-orbit coupling for valence electrons. Orbital moments are mainly described using the spin-orbit coupling treated self-consistently, which is the source of intrinsic magnetic anisotropy, crystal fields are implicitly included in the calculation. Going beyond the single determinant picture is taken somehow into account using non-collinear calculations for magnetic solids within condensed matter codes, a fact that is considered using mixing determinants within quantum chemistry. It is difficult to say which approach is better, but results using both types might be brought into contact when calculations include the required physics and chemistry. Notice that multi-determinant calculations such as CASSCF including all electrons for 3 Ni, 18 C and 18 H atoms seem beyond current computational resources. Last but not least, because we are mainly comparing the ground state properties of two ferromagnetic systems, such as the Ni_3 and Ni_3Bz_3 molecules, density functional theory is perfectly able to deal with the differences⁴¹. Specially, when a study of the Ni_3Bz_3 molecule at this level of theory has not yet been reported. This study should stimulate experimental work toward the synthesis and characterization of the complex.

III. RESULTS AND DISCUSSION

A. Non-spin-orbit calculations

We fully relax Ni_3Bz_3 molecule performing spin-polarized calculations. The ground state is a riceball structure, as shown in Fig. 2. Nickel atoms form an equilateral triangle covered with three benzene molecules, agreeing with experiments²⁰. The nickel-nickel bond lengths are 2.34 Å. The Ni-Ni distances for other nickel-benzene complexes are reported to be close, such as 2.40 Å for Ni_2Bz_2 , 2.45 Å for Ni_3Bz_2 ²⁹, and 2.34 Å for Ni_2Bz_2 ^{24,62}. In comparison, the fully relaxed structure for the bare Ni_3 cluster is an equilateral triangle of side 2.20 Å. The nickel-nickel bonds with Bz molecules enlarge by 0.14 Å (6%). Furthermore, the Ni_3Bz_3 state is ferromagnetic, found 0.2 eV below a spin compensated state. The total spin magnetic moment of Ni_3Bz_3 has 2 μ_B with equal contribution from each of the three nickel atoms. Note that for the bare Ni_3 , a total spin mag-

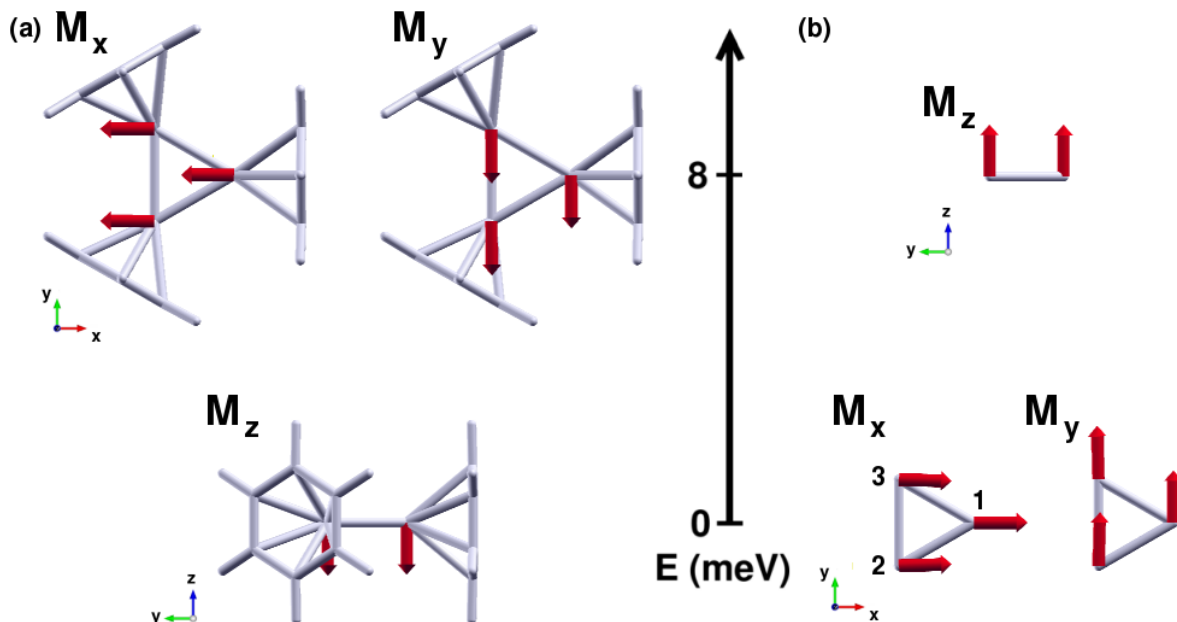


FIG. 2: Energy of different magnetic configurations for (a) Ni_3Bz_3 and (b) Ni_3 . The local Ni spin magnetic moments are denoted by red arrows. Panel of the Ni_3 M_x configuration includes nickel atoms labeled with numbers, which are used for all the configurations of both Ni_3 and Ni_3Bz_3 .

netic moment of $2 \mu_B$ is also reproduced, agreeing with previous reports^{42–48}. Summing up, Ni in the Ni_3Bz_3 metallocene complex is in an oxidation state zero with short Ni-Ni bond lengths and showing ferromagnetic Ni-Ni coupling. The local electronic configuration that in Ni isolated atom is $3d^8 4s^2$ becomes close to $3d^9 4s^1$ in the complex.

B. Spin-orbit calculations

1. Energy and spin magnetic moments

We first explore whether collinear or non-collinear arrangements are preferred by computing different solutions of the local Ni spin magnetic moments. We start with different non-collinear moments in Ni atoms, such as in-plane radial, in-plane tangential, and along xz -diagonals. All these configurations converge to collinear local magnetic moments. The total spin magnetic moment of the ground state of Ni_3Bz_3 remains as $2 \mu_B$ with equal contribution from each Ni atom being ferromagnetically aligned, similar to the spin-polarized results discussed above.

We then include the effects of the relativistic spin-orbit interactions. We align the Ni magnetic moments collinear and sample different in-plane magnetic orientations, for instance along positive and negative directions in the x - and y -axes. Our results show that solutions having the Ni moments in-plane are nearly degenerate, with energy differences smaller than 0.1 meV. We also calculate the case

with the Ni magnetic moments along the z -axis perpendicular to the Ni triangle. In fact, this magnetic solution is the ground state, being 8 meV lower in energy than the in-plane solutions. The local spin magnetic moments are decomposed around Ni atoms as shown in Fig. 2. It is noteworthy that our results reveal a large magnetic anisotropy energy of 8 meV with an easy axis out-of-plane, and a hard plane formed by the three Ni atoms. We define the magnetic anisotropy energy as the difference in energy between in-plane and out-of-plane configurations. The magnetic moments of Ni surrounded by Bz molecules suggest that Ni_3Bz_3 complexes deposited on metallic surfaces could be used as units in magnetic memories useful in data storage applications^{49–51}, although further calculations to evaluate the effect of the substrate are needed.

For comparison we repeat the analysis for the bare Ni_3 molecule to show that benzene molecules are key to get the out-of-plane magnetic configuration. The ground state of Ni_3 is an equilateral triangle with a total spin magnetic moment of $2 \mu_B$. We calculate several arrangements for the local spin magnetic moments by looking for different non-collinear solutions. Nevertheless, our results show that the Ni_3 triangle has collinear magnetic moments, as for Ni_3Bz_3 . Then, we explore the solutions with in-plane and out-of-plane Ni moments. The ground state of Ni_3 is nearly degenerated with several in-plane configurations, with the local Ni magnetic moments parallel pointing either in the x - or y -axis. These in-plane states have similar total energies within an interval of 0.2 meV. The out-of-plane Ni_3 magnetic configuration is about few meV higher in energy than the in-plane

Ni₃ configurations. This result is reversing the magnetic configuration order found for the Ni₃Bz₃ molecule. The addition of Bz molecules to Ni₃ molecule is thus switching the magnetization from the Ni₃ easy xy-plane to the Ni₃Bz₃ easy z-axis.

2. Orbital magnetic moments and experimental considerations

We next have to consider that the total magnetic moment can be decomposed in two contributions, namely the spin magnetic moment and the orbital magnetic moment. We have addressed the spin magnetic moments of Ni atoms above, and we focus on the orbital magnetic moments. The values of the L , S and J operators in each Ni atom of the Ni₃ and Ni₃Bz₃ systems are given in the Supplemental Material. Figure 3 (a) shows the orbital magnetic moments \vec{L} for the different magnetic configurations of the Ni₃Bz₃ molecule. The local Ni orbital magnetic moments nearly follow the direction of the local spin magnetic moments shown in Fig. 2. For the in-plane configurations, the orbital moments of the (2) and (3) Ni atoms are slightly tilted with respect to the local spin magnetic moments.

In comparison, the out-of-plane configuration of Ni₃ has the orbital magnetic moments still aligned with the spin magnetic moments. However, the in-plane orbital magnetic moments of Ni₃ are larger than in Ni₃Bz₃, and rotate from the direction of Ni local spin magnetic moments. For the Ni₃ in-plane configurations there is even a Ni atom with a zero orbital magnetic moment. The orbital moments are averaged within a sphere centered on each Ni atom, so that regions with different moment direction around a Ni atom could cancel and give a total value of nearly zero Ni moment, as seen in the (1) atom of the M_y configuration in Fig. 3.

The spin and orbital magnetic moments of the isolated Ni cluster cations in gas phases with 7-17 atoms have been analyzed using X-ray magnetic circular dichroism (XMCD) spectroscopy⁵². The orbital magnetic moments for these clusters are within the interval 0.25–0.43 μ_B /atom, much larger than the reported 0.06 μ_B /atom for bulk Ni^{53,54}. In agreement with experiments⁵², we find that the local orbital magnetic moments in Ni₃ in-plane configurations have values within the interval 0.23–0.44 μ_B . The orbital magnetic moments increase for small clusters because the crystal field effect decreases in comparison to bulk. However, when comparing to the nickel atom with $\mu_L = 3 \mu_B$, the orbital magnetic moments are considered to be notably quenched, decreasing to 5-25% of the atomic value⁵⁵⁻⁵⁷. For the energetically less stable out-of-plane Ni₃ configuration, the μ_L values decrease even further to 0.06 μ_B .

The out-of-plane Ni₃Bz₃ has slightly larger orbital moments of about 0.12 μ_B . The in-plane configurations of Ni₃Bz₃ also have orbital magnetic moments in the interval 0.05–0.07 μ_B , like in bulk Ni^{53,54}. The ben-

zene molecule addition makes Ni clusters to behave more like bulk Ni because the local orbital magnetic moments decreases^{53,54}. Our results agree with previous reported trends^{55,56}: for bare small nickel clusters orbital magnetic moments are enhanced, and covering with benzenes quenches the orbital magnetic moments because of the induced crystal field, and align them with the spin magnetic moments. Furthermore, we find that the most stable configurations, namely out-of-plane for Ni₃Bz₃ and in-plane for Ni₃, are related to the largest values of the orbital magnetic moments. This finding is in agreement with the reported relationship between orbital magnetic moments and magnetic anisotropy energy⁵⁸⁻⁶⁰.

C. Electronic structure

To understand the effect of the benzene molecules addition, we further study the electronic structure of the Ni₃Bz₃ and Ni₃ clusters. We comment on the spin-orbit calculations to investigate the magnetic anisotropy change upon magnetic fields; non-spin-orbit calculations are commented in the Supplemental Material. Figure 4(a) shows the levels of the M_x and M_z configurations for magnetic fields in the x and z directions, respectively. The M_y configuration behaves similarly to M_x. For the in-plane configurations, either along M_x or M_y, there are two degenerated levels near the Fermi energy, sharing the less bonded electron. Nevertheless, for out-of-plane magnetic moments M_z, these two levels near the Fermi level are no longer degenerated. They present a splitting of more than 24 meV, as indicated by arrows in Fig. 4(a), so the electron fills the lower energy level. This degeneration breaking stabilizes the out-of-plane Ni₃Bz₃ configuration (M_z) with respect to in-plane cases (M_x or M_y) by more than 8 meV.

Next, we compare with the corresponding Ni₃ levels. Figure 4(b) shows the levels of the M_x and M_z configurations for magnetic fields in the x and z directions, respectively. The M_y configuration behaves similarly to M_x. Regarding stability, Ni₃ in-plane configurations are 8 meV more stable than the out-of-plane configuration, in contrast to Ni₃Bz₃. The in-plane configurations have the two levels near the Fermi energy fully occupied and almost degenerated, with a small splitting of 8 meV. In the out-of-plane case the splitting between the two fully occupied levels becomes as large as 56 meV, a value that is about double than for Ni₃Bz₃. Out-of-plane magnetic field favors the splitting, as for Ni₃Bz₃.

Nevertheless, there is an important difference between the Ni₃Bz₃ and Ni₃ cases; two electrons fills these two levels for Ni₃ while only one electron is available for the Ni₃Bz₃ couple of levels. For Ni₃Bz₃ in-plane configurations, the two levels near the Fermi energy share an electron, which is a destabilizing factor. The out-of-plane magnetic field splits these two levels enabling complete filling of one of them, stabilizing the Ni₃Bz₃ molecule. This explains the switch of the easy axis between Ni₃

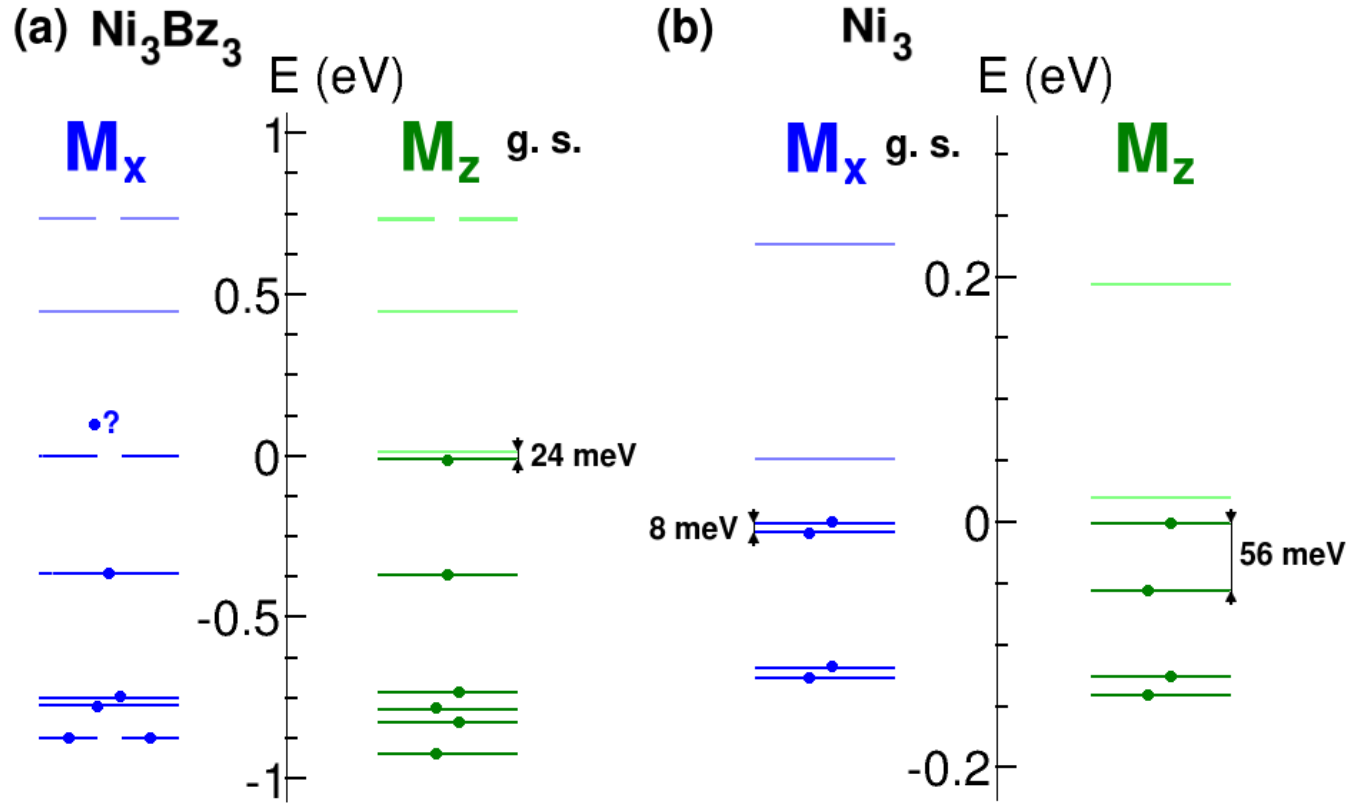
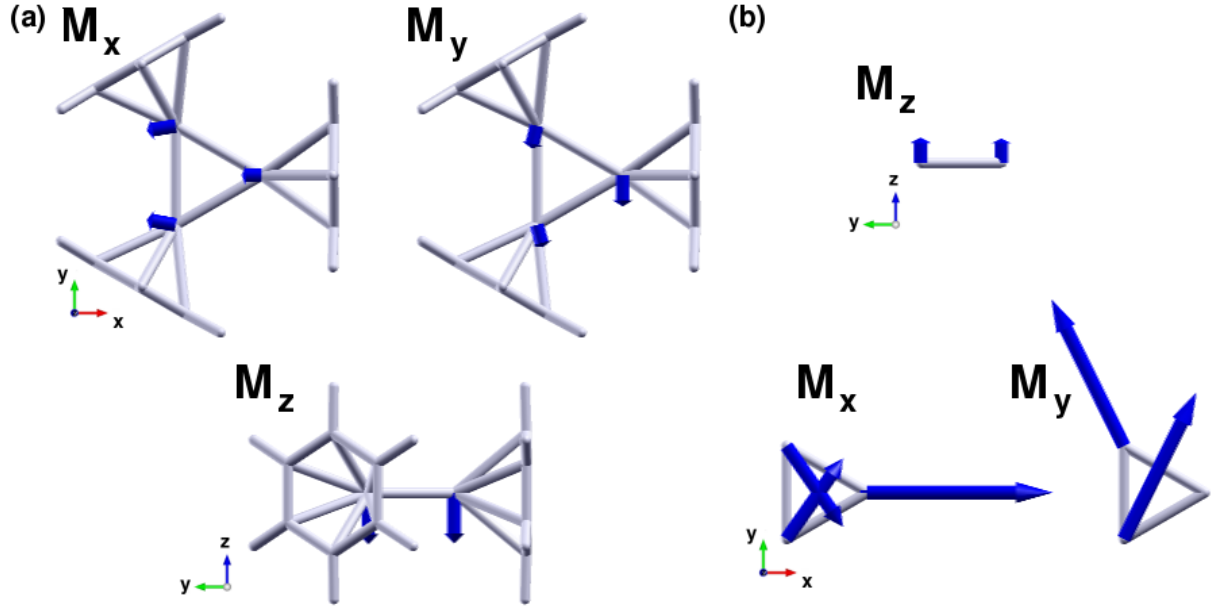


FIG. 4: Electronic levels near the Fermi energy obtained in spin-orbit (SO) calculations for the (a) Ni_3Bz_3 and (b) Ni_3 molecules.

and Ni_3Bz_3 .

Finally, we searched for the cause of the difference number of electrons in these two levels near the Fermi energy between Ni_3 and Ni_3Bz_3 . The role of benzenes reveals as key for the magnetic change. The addition of benzene molecules leads to charge transfer towards nickel atoms⁶³ and symmetrizes the system, stabilizing and filling a 4s level for Ni_3Bz_3 , which is unoccupied for Ni_3 . Consequently, the couple of degenerated levels at the Fermi energy for Ni_3Bz_3 becomes half-occupied by an electron.

IV. CONCLUSIONS

We here performed spin-orbit calculations for organometallic compounds containing benzene molecules and nickel atoms. We find that molecules Ni_3Bz_3 begin to behave as small magnets with all the Ni atom moments being collinear. The effect of benzene molecules is to switch the easy axis of magnetization from in-plane (for the bare nickel cluster Ni_3) to out-of-plane (for molecule Ni_3Bz_3). The in-plane magnetic configurations for molecule Ni_3Bz_3 , being almost degenerated, are 8 meV higher in energy than the out-of-plane magnetic configuration, a finding that shows a large magnetic

anisotropy energy. The out-of-plane easy axis correlates with the large values of the Ni orbital magnetic moments. The switching of the easy axis between the bare and covered Ni_3 clusters is explained using the different occupation of two degenerated levels near the Fermi energy, which are split by an applied perpendicular out-of-plane magnetic field. Thus, small Ni_3Bz_3 magnetic molecules could be of use in applications as magnetic memories because of the large magnetic anisotropy energy with the out-of-plane easy axis, magnetic properties that are further ensured by the protection provided by the embedding of benzene molecules.

Acknowledgement

This work was part financed by the Project FIS2016-76617-P of the Spanish Ministry of Economy and Competitiveness MINECO, the Basque Government under the ELKARTEK project (SUPER), and the University of the Basque Country (Grant No. IT-756-13). TALL acknowledges a grant provided by the MPC Material Physics Center - San Sebastián. The authors also acknowledge the technical support of the DIPC computer center. We acknowledge Prof. Andrei Postnikov for reading the manuscript.

-
- ¹ T. Kealy and P. Pauson, *Nature* **168**, 1039 (1951).
 - ² F. N. Pansini and F. A. de Souza, *J. Phys. Chem. A* **120**, 2771 (2016).
 - ³ Y. Zeng, H. Feng, R. B. King, and H. F. Schaefer III, *Organometallics* **33**, 7193 (2014).
 - ⁴ J.-X. Yu, J. Chang, R.-K. Wei, X.-Y. Liu, and X.-D. Li, *Phys. E* pp. 294–297 (2016).
 - ⁵ R. Liu, S.-H. Ke, W. Yang, and H. U. Baranger, *J. Chem. Phys.* **127**, 141104 (2007).
 - ⁶ R. Liu, S.-H. Ke, H. U. Baranger, and W. Yang, *Nano Lett.* **5**, 1959 (2005).
 - ⁷ C. Timm and F. Elste, *Phys. Rev. B* **73**, 235304 (2006).
 - ⁸ C. Ornelas, *New J. Chem.* **35**, 1973 (2011).
 - ⁹ S. Gomez-Ruiz, D. Maksimović-Ivanić, S. Mijatović, and G. N. Kaluderović, *Bioinorg. Chem. Appl.* **2012** (2012).
 - ¹⁰ X. Li, L. M. Guard, J. Jiang, K. Sakimoto, J.-S. Huang, J. Wu, J. Li, L. Yu, R. Pokhrel, G. W. Brudvig, et al., *Nano Lett.* **14**, 3388 (2014).
 - ¹¹ A. Ishii and T. Miyasaka, *ChemPhysChem* **15**, 1028 (2014).
 - ¹² K. Park, S. Oh, D. Jung, H. Chae, H. Kim, and J.-H. Boo, *Nanoscale Res. Lett.* **7**, 1 (2012).
 - ¹³ K. M. Wedderburn, S. Bililign, M. Levy, and R. J. Gdanitz, *Chem. Phys.* **326**, 600 (2006).
 - ¹⁴ R. Pandey, B. K. Rao, P. Jena, and M. A. Blanco, *J. Am. Chem. Soc.* **123**, 3799 (2001).
 - ¹⁵ R. Pandey, B. Rao, P. Jena, and J. M. Newsam, *Chem. Phys. Lett.* **321**, 142 (2000).
 - ¹⁶ R. Muhida, W. Agerico Diño, M. Mahmudur Rahman, H. Kasai, and H. Nakanishi, *J. Phys. Soc. Jpn.* **73**, 2292 (2004).
 - ¹⁷ K. Miyajima, S. Yabushita, M. B. Knickelbein, and A. Nakajima, *J. Am. Chem. Soc.* **129**, 8473 (2007).
 - ¹⁸ M. A. Duncan, *Int. J. Mass spectrom.* **272**, 99 (2008).
 - ¹⁹ W. Zheng, J. M. Nilles, O. C. Thomas, and K. H. Bowen, *J. Chem. Phys.* **122**, 44306 (2005).
 - ²⁰ T. Kurikawa, H. Takeda, M. Hirano, K. Judai, T. Arita, S. Nagao, A. Nakajima, and K. Kaya, *Organometallics* **18**, 1430 (1999).
 - ²¹ F. Rabilloud, *J. Chem. Phys.* **122**, 134303 (2005).
 - ²² R. Flores and M. Castro, *J. Mol. Struct.* **1125**, 47 (2016).
 - ²³ G. E. Froudakis, A. N. Andriotis, and M. Menon, *Chem. Phys. Lett.* **350**, 393 (2001).
 - ²⁴ J. Zhou, W.-N. Wang, and K.-N. Fan, *Chem. Phys. Lett.* **424**, 247 (2006).
 - ²⁵ D. Rayane, A.-R. Allouche, R. Antoine, M. Broyer, I. Compagnon, and P. Dugourd, *Chem. Phys. Lett.* **375**, 506 (2003).
 - ²⁶ J. W. Gonzalez, T. Alonso-Lanza, F. Delgado, F. Aguilera-Granja, and A. Ayuela, *Phys. Chem. Chem. Phys.* **19**, 14854 (2017).
 - ²⁷ T. Alonso-Lanza, J. W. González, F. Aguilera-Granja, and A. Ayuela, *J. Phys. Chem. C* **121**, 25554 (2017).
 - ²⁸ R. Xiao, D. Fritsch, M. D. Kuzmin, K. Koepf, H. Eschrig, M. Richter, K. Vietze, and G. Seifert, *Phys. Rev. Lett.* **103**, 187201 (2009).
 - ²⁹ B. Rao and P. Jena, *J. Chem. Phys.* **116**, 1343 (2002).
 - ³⁰ P. E. Blöchl, *Phys. Rev. B* **50**, 17953 (1994).
 - ³¹ G. Kresse and D. Joubert, *Phys. Rev. B* **59**, 1758 (1999).
 - ³² J. P. Perdew, K. Burke, and M. Ernzerhof, *Phys. Rev. Lett.* **77**, 3865 (1996).
 - ³³ J. M. Soler, E. Artacho, J. D. Gale, A. García, J. Jun-

- quera, P. Ordejón, and D. Sánchez-Portal, J. Phys. Condens. Matter **14**, 2745 (2002).
- ³⁴ N. Troullier and J. L. Martins, Phys. Rev. B **43**, 1993 (1991).
- ³⁵ L. Kleinman and D. Bylander, Phys. Rev. Lett. **48**, 1425 (1982).
- ³⁶ T. Alonso-Lanza, A. Ayuela, and F. Aguilera-Granja, Phys. Chem. Chem. Phys. **18**, 21913 (2016).
- ³⁷ *Elk*, <http://elk.sourceforge.net/> (2010), all-electron full-potential linearised augmented-plane wave (FP-LAPW) code.
- ³⁸ D. J. Singh and L. Nordstrom, *Planewaves, Pseudopotentials, and the LAPW method* (Springer Science & Business Media, 2006).
- ³⁹ E. Sjöstedt, L. Nordström, and D. Singh, Solid State Commun. **114**, 15 (2000).
- ⁴⁰ U. von Barth and L. Hedin, J. Phys. C: Solid State Phys. **5**, 1629 (1972).
- ⁴¹ A. V. Postnikov, J. Kortus, and M. R. Pederson, physica status solidi (b) **243**, 2533 (2006).
- ⁴² M. Michelini, R. Pis Diez, and A. Jubert, Int. J. Quantum Chem. **70**, 693 (1998).
- ⁴³ B. N. Papas and H. F. Schaefer III, J. Chem. Phys. **123**, 074321 (2005).
- ⁴⁴ M. Castro, C. Jamorski, and D. R. Salahub, Chem. Phys. Lett. **271**, 133 (1997).
- ⁴⁵ G. A. Cisneros, M. Castro, and D. R. Salahub, Int. J. Quantum Chem. **75**, 847 (1999).
- ⁴⁶ Z. Xie, Q.-M. Ma, Y. Liu, and Y.-C. Li, Phys. Lett. A **342**, 459 (2005).
- ⁴⁷ G. L. Arvizu and P. Calaminici, J. Chem. Phys. **126**, 194102 (2007).
- ⁴⁸ M. Michelini, R. P. Diez, and A. Jubert, Comput. Mater. Sci. **31**, 292 (2004).
- ⁴⁹ T. Choi, W. Paul, S. Rolf-Pissarczyk, A. J. Macdonald, F. D. Natterer, K. Yang, P. Willke, C. P. Lutz, and A. J. Heinrich, Nat. Nanotechnol. pp. 420–424 (2017).
- ⁵⁰ C. Chappert, A. Fert, and F. N. Van Dau, Nat. Mater. **6**, 813 (2007).
- ⁵¹ A. R. Rocha, V. M. Garcia-Suarez, S. W. Bailey, C. J. Lambert, J. Ferrer, and S. Sanvito, Nat. Mater. **4**, 335 (2005).
- ⁵² J. Meyer, M. Tombers, C. van Wüllen, G. Niedner-Schatteburg, S. Peredkov, W. Eberhardt, M. Neeb, S. Palutke, M. Martins, and W. Wurth, J. Chem. Phys. **143**, 104302 (2015).
- ⁵³ J. Vogel and M. Sacchi, Phys. Rev. B **49**, 3230 (1994).
- ⁵⁴ C. Chen, N. Smith, and F. Sette, Phys. Rev. B **43**, 6785 (1991).
- ⁵⁵ C. Kittel, *Introduction to solid state physics* (Wiley, 2005).
- ⁵⁶ J. Stöhr and H. C. Siegmann, *Magnetism: from fundamentals to nanoscale dynamics*, vol. 152 (Springer Science & Business Media, 2007).
- ⁵⁷ A. Langenberg, K. Hirsch, A. Lawicki, V. Zamudio-Bayer, M. Niemeyer, P. Chmiela, B. Langbehn, A. Terasaki, B. v. Issendorff, and J. Lau, Phys. Rev. B **90**, 184420 (2014).
- ⁵⁸ P. Bruno, Phys. Rev. B **39**, 865 (1989).
- ⁵⁹ L. M. Liz-Marzán and P. V. Kamat, *Nanoscale Materials* (Springer, 2003).
- ⁶⁰ H. Hopster and H. P. Oepen, *Magnetic Microscopy of Nanostructures*, NanoScience and Technology (Springer Berlin Heidelberg, 2006).
- ⁶¹ B. P. Stoicheff, Can. J. Phys. **32**, 339 (1954).
- ⁶² The distances between each nickel and the six nearest carbon atoms of the benzene molecule have about 2.21 Å, a value which should be compared well with the 2.04–2.21 Å interval for Ni₂Bz₂, and with 2.08 Å for Ni₃Bz₂²⁹ and 2.14–2.34 Å for Ni₂Bz₂²⁴, cases in which the nickel atom is not even η^6 -bonded. The carbon-carbon bond length is 1.41 Å as found in experiments 1.40 Å⁶¹.
- ⁶³ Considering the charge transfer under the Mulliken scheme, we find that for the Ni₃Bz₃ molecule, each nickel atoms gains more than 0.2 electrons. In total, the three nickel have 0.65 electrons, in agreement with findings for molecule Co₃Bz₃²⁶.

Supporting Information: Out-of-plane Enhanced Magnetic Anisotropy Energy in Ni₃Bz₃ molecule

SI. MAGNITUDES OF THE QUANTUM NUMBERS

Tables S1 and S2 include the magnitudes of the angular moments L , S and J for Ni₃ and Ni₃Bz₃. It is noteworthy that the L values for Ni₃ in in-plane configurations are comparable to the S values. The addition of benzene molecules decreases the L value. For Ni₃Bz₃ and Ni₃, the largest local orbital magnetic moments are found for the most stable out-of-plane and in-plane configurations, respectively.

TABLE S1: Values of the L , S and J angular moments in each of the atom spheres for the three different magnetic configurations found for the Ni₃ molecule.

	M _x			M _y			M _z		
	1	2	3	1	2	3	1	2	3
L	0.44	0.23	0.23	0.01	0.39	0.39	0.06	0.06	0.06
S	0.34	0.34	0.34	0.33	0.34	0.34	0.33	0.33	0.33
J	0.78	0.51	0.51	0.34	0.71	0.71	0.39	0.39	0.39

TABLE S2: Values of the L , S and J angular moments in each of the atom spheres for the three different magnetic configurations found for the Ni₃Bz₃ molecule.

	M _x			M _y			M _z		
	1	2	3	1	2	3	1	2	3
L	0.05	0.07	0.07	0.07	0.05	0.05	0.12	0.12	0.12
S	0.34	0.35	0.35	0.34	0.35	0.35	0.34	0.35	0.35
J	0.39	0.42	0.42	0.41	0.40	0.40	0.46	0.47	0.47

SII. NON-SPIN-ORBIT ELECTRONIC STRUCTURE

Figure S1 displays the electronic levels for non-spin-orbit calculations of (a) Ni₃Bz₃ and (b) Ni₃ molecules. For the Ni₃Bz₃ molecule, the highest occupied molecular orbital (HOMO) for the minority spin is a doubly degenerated level occupied by an electron. The wave functions

of these two levels, displayed nearby, show that they are mainly formed by a combination of d_{xz} and d_{yz} atomic orbitals in each Ni atom. The specific orbital composition of those levels is studied by the projected-density-of-states also shown in the Supplemental Material. In the case of Ni₃, there are two minority spin levels degenerated at the Fermi energy as for Ni₃Bz₃, however each level is totally filled with an electron. Their wave functions have d orbital contribution with strong z component, as for Ni₃Bz₃. These results agree with those of spin-orbit calculations.

SIII. PROJECTED DENSITY OF STATES

Figure S2 shows the projected density of states (PDOS) over C and Ni orbitals for (a) Ni₃Bz₃ and (b) Ni₃ molecules. The coordinate system is the same as used in the main article. We first comment the PDOS results of Ni₃Bz₃ in panel (a). The spin splitting for the d levels near the Fermi energy is estimated about 1 eV. Carbon contributions expand over almost all the energies, hybridizing with nickel orbitals. The Ni d orbital contributions are brought together into couples, such as $3d_{xz}$ - $3d_{yz}$ and $3d_{xy}$ - $3d_{x^2-y^2}$, because the hybridized molecular orbitals have contributions with similar weights at the same energies. The couple $3d_{xz}$ - $3d_{yz}$ form molecular orbitals in the out-of-plane z -direction, and the second couple $3d_{xy}$ - $3d_{x^2-y^2}$ forms orbitals in the Ni atom plane. Near the Fermi energy, there are two minority spin levels composed of hybridizing $3d_{xz}$ - $3d_{yz}$ Ni orbitals, which are occupied by one electron and are responsible for the magnetic anisotropy of Ni₃Bz₃.

Second we discuss the projected density of states for Ni₃ (see Fig. S2(b)). The scheme of hybridization between d orbitals is the same as for Ni₃Bz₃. However, the two occupied degenerated levels near the Fermi energy are totally filled, as shown in the level schemes in the main article. The contributions of $4s$ and $3d_{z^2}$ orbitals show differences between Ni₃ and Ni₃Bz₃ near the Fermi energy. The $4s$ orbital for Ni₃ is highly hybridized with the $3d_{xy}$ - $3d_{x^2-y^2}$ couple and $3d_{z^2}$ orbital contributions. The addition of benzene molecules localize a molecular orbital composed of d_{z^2} Ni, that for the Ni₃Bz₃ molecule is being shifted towards deeper energies together with the $4s$ contribution. It is noteworthy that for Ni₃Bz₃ a level composed of $4s$ Ni appears about 1 eV below the Fermi energy.

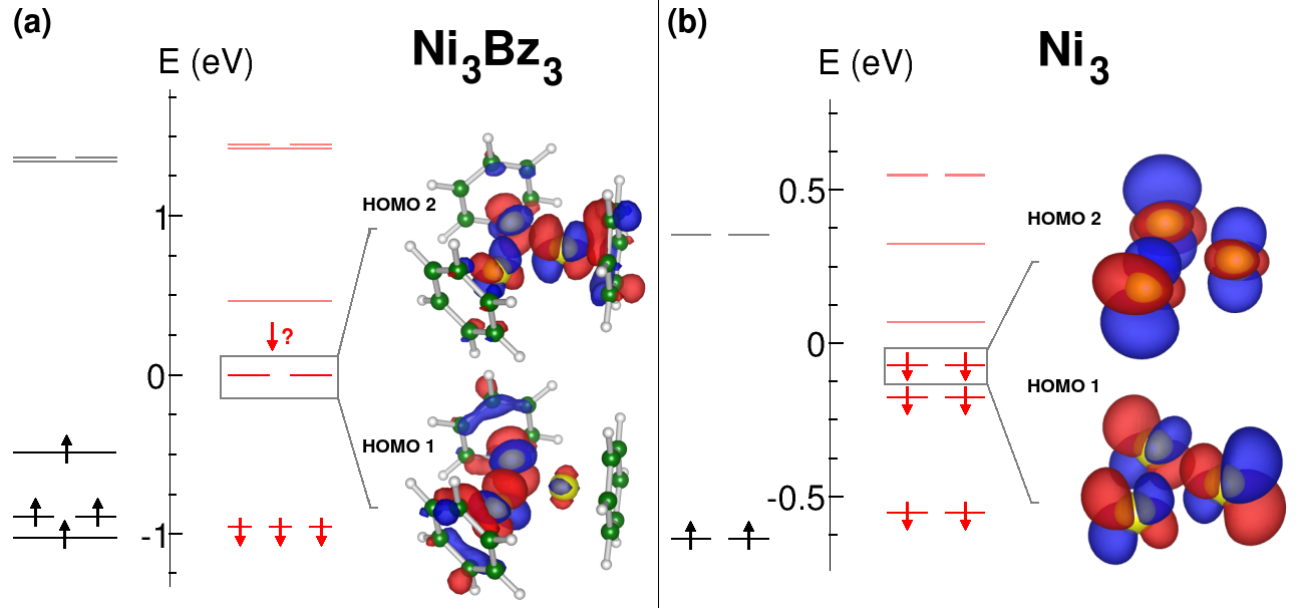


FIG. S1: Electronic levels obtained with non spin-orbit calculations for the (a) Ni_3Bz_3 and (b) Ni_3 molecules. The wavefunctions of the down levels at the Fermi energy are displayed.

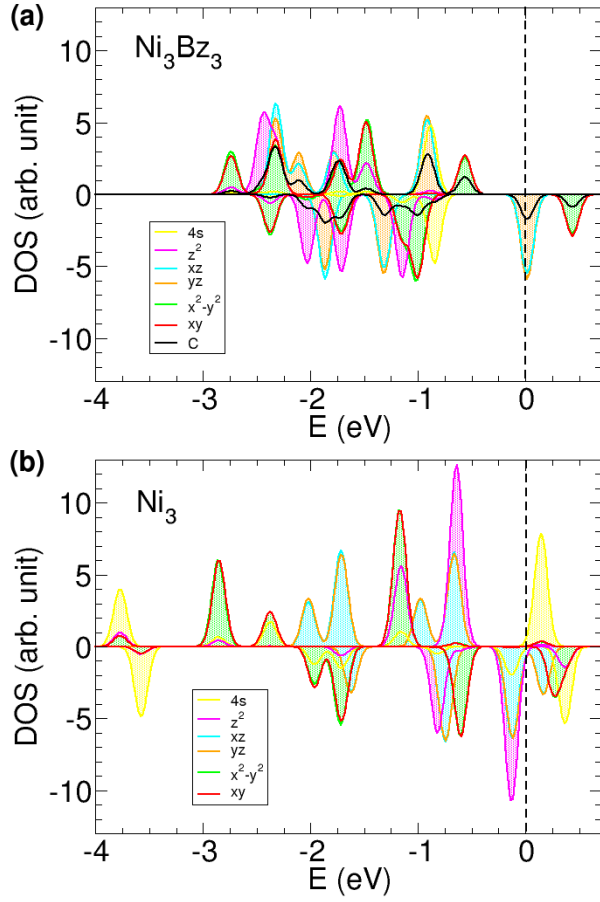


FIG. S2: Projected density of states for (a) Ni_3Bz_3 and (b) Ni_3 .